Published in final edited form as:
J Am Chem Soc. 2009 October 28; 131(42): 15492–15500. doi:10.1021/ja9066282.

Synthesis of highly enantioenriched 3,4-dihydroquinolin-2-ones by 6-*exo-trig* radical cyclizations of axially chiral α-halo-*ortho*-alkenyl anilides

David B. Guthrie, **Steven J. Geib**, and **Dennis P. Curran***
Department of Chemistry, University of Pittsburgh, Pittsburgh PA, 15260 USA

Abstract

Radical cyclizations (Bu_3SnH, Et_3B/air, rt) of racemic α-halo-*ortho*-alkenyl anilides provide 3,4-dihydroquinolin-2-ones in high yield. Cyclizations of enantioenriched precursors occur in similarly high yields and with transfer of axial chirality to the new stereocenter of the products with exceptionally high fidelity (often > 95%). Single and tandem cyclizations of α-halo-*ortho*-alkenyl anilides bearing an additional substituent on the α-carbon occur with high chirality transfer and high diastereoselectivity. Straightforward models are proposed to interpret both the chirality transfer and diastereoselectivity aspects. These first examples of an approach for axial chiral transfer from a reactive species in the amide to an acceptor suggest broad potential for extension both within and beyond radical reactions.

Introduction

The dihydroquinolin-2-one ring is an important heterocycle that is featured in both natural products and medicinally active compounds.[1] Dihydroquinolin-2-ones can exist as isolated ring systems, as in the penigquinolones,[2] pinolinone,[3] $\alpha_2\beta_3$ integrin antagonists[4] (see **1**, Figure 1), and a class of HIV reverse transcriptase inhibitors.[5] Or, they can be conjoined with other rings, as in scandine and the related meloscine alkaloids (see **2**, Figure 1).[6,7] Many methods exist to make racemic dihydroquinolin-2-ones, but only a few routes toward single enantiomers have been reported.[8] These methods suffer from various drawbacks (low ee, limited generality), so new methods are needed.

Many of the most important dihydroquinolin-2-ones have alkyl or other substituents at the C-4 position, and convenient ways to access such compounds in racemic form involve 6-*exo-trig* cyclizations. Figure 2 shows examples of both radical[9] and ionic approaches. Jones reported that reduction of **3** with Bu_3SnH provided target dihydroquinolin-2-one **4** along with comparable amounts of the product of 1,5-hydrogen transfer **5** in 51% combined yield.[10] In this method (Approach 1), a radical generated on the aryl ring cyclizes to an acceptor on the anilide carbonyl group. Ikeda[11] and Parsons[12] took the reverse strategy (Approach 2), generating a radical adjacent to the amide carbonyl group and allowing it to cyclize onto an alkene at the *ortho* position of the aryl ring. For example, cyclization of **6** under syringe pump conditions provided **7** in 79% isolated yield.

curran@pitt.edu.

SUPPORTING INFORMATION AVAILABLE: Contains procedures of synthesis and characterization data of all new compounds and copies of NMR spectra. This material is available free of charge via the Internet at http://pubs.acs.org.

Cyclization strategies towards these targets are not limited to radical approaches. Procter and coworkers have developed a general approach to racemic dihydroquinolin-2-ones by using intramolecular conjugation addition of α-arene sulfonyl anilides.[13] For example, base-promoted cyclization of **8** followed by reductive desulfonylation with samarium diiodide provided **9** in 57% yield. α-Alkylation can be conducted between the cyclization and the desulfonylation steps to provide products with substitution at C-3. The sulfone can also be grafted to a polymer bead for solid phase synthesis.

It is now widely recognized that *ortho*-substituted anilides like **3**, **6** and **8** are not planar, as implied by the two-dimensional drawings in Figure 2. Instead, the planes of the amide group and the aryl ring are roughly orthogonal, as shown by the structures in Figure 3.[14] Accordingly, the molecules are axially chiral, and stable atropisomers result with suitable substitution patterns.[15] With such molecules, cyclizations (radical or otherwise) might occur with transfer of axial chirality to give a product whose configuration is predetermined by that of the starting material.[16] For example, tin hydride cyclizations of *o*-iodoacrylanilides **10** provide indol-2-ones **11** in high yields with excellent levels of chirality transfer. The scope of this radical reaction is excellent, and anionic[17] and organometallic[18] variants also exist. Because this produces an indol-2-one rather than a dihydroquinolin-2-one, this reaction can be viewed as a lower homolog of Approach 1 in Figure 2.

However, in assessing prospects for making dihydroquinolin-2-ones by axial chirality transfer, we felt that Approach 2 was considerably more interesting than Approach 1 for three reasons. First, the scope and generality of Approach 1 may be limited; β,γ-unsaturated amides like **12** are not as easy to make or handle as α,β-unsaturated analogs, and the competing 1,5-hydrogen transfer reaction that these substrates permit (see **13**) could be a fatal design flaw in many cases.[19] Second, Approach 2 represents a potentially new class of chirality transfer reaction for axially chiral anilides. In all previous reactions, a reactive intermediate (radical, anion, metal) on the aryl ring is generated first, and reacts in turn with an acceptor in a pendant side chain on the amide. Is it possible to reverse the roles of the two partners without sacrificing the high chirality transfer?

The third reason has to do with N–Ar bond rotation, which must be avoided because it results in racemization. Consider the generation of radical **13** from **12** in Approach 1. This event must cause a significant decrease in the N–Ar rotation barrier because one of the *ortho*-substituents is now a radical, which is much smaller than its precursor. In contrast, the N–Ar rotation barriers of precursor **15** and radical **16** in Approach 2 are likely comparable because their substitution patterns are very similar. Even so, strict prevention of N–Ar bond rotation is a necessary but not sufficient condition for axial chirality transfer. Addition to the alkene must also be face selective, as must addition to the radical (rho selectivity) if it has three different substituents (this later selectivity is not illustrated in Figure 3 because the radical has two hydrogen atoms).

Here we report details of an in-depth study of 6-*exo*-*trig* radical cyclizations of both racemic and enantiopure axially chiral α-halo-*ortho*-alkenyl anilides. Dihydroquinolin-2-ones are formed in good yields, and with exceptionally high fidelity in transfer of axial chirality. As a bonus, the reactions of alkyl-substituted amide radicals are also highly diastereoselective. These first results suggest that there is excellent potential to extend Approach 2 for axial chirality transfer both within and beyond radical reactions.

Results and Discussion

Synthesis of Radical Cyclization Precursors

An initial set of nine radical cyclization precursors **15a-i** (Table 1) was prepared in racemic form to assess the efficiency of the radical cyclization as a function of substituent pattern. The

synthesis of **15a** is typical, and is summarized in Scheme 1. Heck reaction of 2-iodo-*N*,4,6-trimethylaniline **17**[16e] with *t*-butyl acrylate under ligand-free conditions[20] provided **18a** in 92% yield. Acylation of **18a** with chloroacetyl chloride gave α-chloro anilide **19a** in 90% yield. This was converted to the α-iodoanilide **15a** by Finkelstein reaction in 93% yield. The syntheses of all the precursors **15a-i** are described in detail in the Supporting Information. Most pathways were similar to Scheme 1, with suitable variations for substrate. Other protocols were sometimes used for the Heck reaction,[21] and the trisubstituted alkene of **15i** was appended by Negishi coupling.[22]

Cyclizations of Racemic Precursors

Table 1 compiles the key results of cyclization experiments conducted under a standard set of conditions. In a typical experiment, Bu_3SnH and Et_3B initiator[23] were dissolved in degassed PhH, and this solution was added dropwise by syringe pump over 2 h to a non-degassed PhH solution of substrate **15a** at room temperature. TLC analysis showed that the reaction was complete at the end of the addition period. The solvent was removed, and the crude mixture was directly chromatographed on 10% w/w KF/silica gel.[24] This removed the tin byproducts and at the same time purified the target product **14a**, which was isolated in 83%. A similar experiment at a fixed Bu_3SnH concentration of 10 mM was complete in 5 min, but provided only 55% yield of a sample of **14a** that was not completely separable from the directly reduced product **20a**.

Substrate **15b,** with an *N*-*p*-methoxybenzyl (PMB) substituent, provided product **14b** in 83% purified yield. The *ortho* substituent was also varied in this series to include methoxy (**15c**, lacking the *p*-methyl group), trimethylsilyl (TMS, **15e**) and bromine (**15f**) while holding the *N*-PMB group and the acceptor constant. The corresponding products **14c,e,f** were isolated in 97, 93 and 61% yields. The TMS group of **14e** survived chromatography over KF-doped silica gel.

The substituents on the acceptor were also changed to *p*-bromophenyl (**15g**), cyano (**15h**) and dimethyl (**15i**). Reduction of the *p*-bromophenyl substrate **15g** provided a complex product mixture that did not obviously contain the expected product **14g** or the reduced product **20g**. The aryl bromide of **15g** is probably not the culprit for this failure, because bromide **15f** cyclized smoothly. Instead, we speculate that the benzyl radical resulting from cyclization will not react quickly enough with tin hydride under these conditions (low concentration and temperature),[25] and instead finds other pathways. Reduction of nitrile **15h** under the syringe pump conditions provided product **14h** in about 70% yield but in unsatisfactory purity even after chromatography. A similar experiment conducted at fixed 5 mM concentration gave the same product in about the same yield, but now the purity was considerably better (95% estimated). The dimethyl substrate **15i** provided pure **14i** in 51% isolated yield. Small amounts of the directly reduced product were also produced, presumably because the alkene of **15i** is not as good of a radical acceptor as the other alkenes.

Finally, a tosyl group was also probed as the *N*-substituent, but reduction of **15d** gave a mixture of products whose major component (~80%) was the directly reduced product **20d**. This failure is surprising since *N*-tosyl groups have been used in the past to facilitate cyclizations of α-amidoyl radicals.[26]

Rate constant measurements

The necessity of syringe pump conditions to minimize premature reduction in reactions of compounds **15** implies a relatively low rate constant for 6-*exo*-*trig* cyclization. This is not surprising since 6-heptenyl radicals typically cyclize more slowly than analogous 5-hexenyl ones. All the atoms connecting the radical precursor and radical acceptor are sp^2-hybridized

in **15**, so estimating rate constants by analogy to other hexenyl and heptenyl radicals is risky. Therefore, we undertook kinetic competition experiments[27] to determine the cyclization rate constant k_c for the reaction of a representative compound **15b**.

The mechanistic framework for the rate constant analysis is shown in Figure 4. Radical **16b** derived from **15b** can be directly reduced in a bimolecular reaction with tin hydride to give **20b**. Alternatively, it can undergo 6-*exo* cyclization to provide a new radical **21b**, which in turn reacts with tin hydride to give **14b**. Measurement of the ratio of cyclized **14b** to reduced **20b** products as a function of tin hydride concentration provides the rate constant k_c in the usual way.[27]

The competition experiments were performed by mixing stock benzene solutions (non-degassed) of **15b** (0.025 mmol), Bu_3SnH (0.030 mmol), and eicosane (internal GC standard) in round bottom flasks open to air. A hexane solution of Et_3B (0.010 mmol) was added all at once. The reaction mixtures were stirred for 10 min, and were then subjected to GC analysis without workup to provide standardized yields of **14b** and **20b**. The average results of three trials at each concentration are summarized in Table 2, and the usual kinetic competition plot of this data is shown in Figure 5. Reactions were complete, reproducible, high-yielding (76–95%), and clean (no significant side peaks in GC analysis) in all cases.

By using the estimated value $k_H = 2.3 \times 10^6\ M^{-1}s^{-1}$ for radical **16b**,[28] we calculated k_c at 25 °C as $8 \times 10^4\ s^{-1}$. This value is about an order of magnitude higher than that for the 6-*exo* cyclization of the 6-heptenyl radical,[27] presumably due to the activating effect of the ester on the alkene. It is coincidentally close to the rate constant for 5-*exo* cyclization of the 5-hexenyl radical ($1 \times 10^5\ s^{-1}$), a value that synthetic chemists often use as a touchstone for radical cyclizations of intermediate rate.

The intercept of a plot of data for an irreversible cyclization should be zero, but the intercept in Figure 5 appears to be slightly positive. This raises the possibility that the cyclization of **16b** may be reversible. From the value of the intercept, we calculated that the ring opening rate constant of k_{-c} of **21b** must be at least 25 times slower than cyclization, so the back cyclization can probably be neglected for most practical purposes. Even so, most 6-*exo* cyclizations to activated alkenes are irreversible.[29] We speculate that the unfavorable 1,3-steric interactions between the *N*-substituent and the substituent of C-8 of the cyclized intermediate **21b** (see Figure 4) may both retard the cyclization and promote the reverse reaction.

Resolution and measurements of rotation barriers

To perform the chirality transfer experiments, we secured highly enantioenriched samples of seven of the precursors by resolution on semipreparative chiral HPLC. Typically, samples of **15** were dissolved in *i*-PrOH, and injected onto either a Chiralcel OD or (*S*,*S*)-Whelk-O 1 column (25.0 cm × 21.1 mm ID) and eluted with a hexane:*i*-PrOH solvent mixture. Depending on the ease of separation, samples ranging in size from 40–120 mg were resolved per injection. After fraction collection and solvent removal, the enantiomeric ratios of the resolved compounds were measured by analytical chiral HPLC. Six of the compounds exhibited the expected two peaks for the individual enantiomers, which were isolated in > 98% ee.

The HPLC behavior of *N*-methyl congener **15a** was an interesting exception. This exists as a 94/6 ratio *E*:*Z* of amide rotamers as assessed by ^1H NMR analysis (see Figure 6). The amide rotamers are visible by silica TLC analysis, but not isolable under ambient laboratory conditions. Analytical HPLC (Whelk, 80:20 hexanes:*i*-PrOH) of the sample showed a small peak at 10.5 min, followed by two large peaks at 14.5 min and 18.5 min. Analysis of the resolved fractions allowed interpretation of this chromatogram. The peak at 10.5 min is the minor Z-amide rotamer of (−)-**15a**, while the major E amide rotamer of (+)-**15a** elutes at 14.5 min. The

minor Z amide rotamer of (+)-**15a** and the major E amide rotamer of (−)-**15a** overlap at 18.1 min. A plateau between the minor and major amide rotamer peaks of each enantiomer shows partial interconversion on the timescale of the HPLC separation. Based on this behavior, we estimate that the barrier for E/Z rotation is in the vicinity of $\Delta G^{\ddagger}_{E/Z} \approx 22$ kcal/mol. This barrier is considerably higher than that for typical amides;[30] however, E/Z rotamers of anilides with even larger ortho substituents have even higher barriers and can be separated and handled at ambient temperature.[31] This effect complicates the measurement of the enantiomer ratio (er) of resolved **15a**, but the relatively small proportion of the minor Z rotamer (6%) minimizes any error.

The other samples with *N*-PMB groups instead of the *N*-Me group did not have significant amounts of the Z rotamer at equilibrium according to analysis of their ^{1}H NMR spectra (E/Z >98/2), and their resolutions were straightforward. Like **15a**, these samples probably have a substantial barrier to E/Z rotation, but the population of the Z rotamer is so low at equilibrium that it can be neglected entirely.

Small samples of four substrates bearing *N*-PMB groups were then racemized to measure their respective barriers to *N*-aryl bond rotation. The samples were dissolved in 90:10 hexane:*i*-PrOH and heated in a sealed tube at an appropriate temperature. Racemization was monitored by periodically measuring the er of aliquots of the solution by analytical chiral HPLC. The experimental data and details of the standard analysis are in the Supporting Information.

The newly measured rotation barriers are summarized in Figure 7 along with benchmarks **22** and **23** from previous work in our group.[16d,e] The barrier to rotation of *o*-methyl substrate **15b** was $\Delta G^{\ddagger}_{rot} = 34.3$ kcal/mol, while the *o*-Br substrate **15f** had a similar barrier of 34.2 kcal/mol. The magnitudes of these barriers are surprisingly high when contrasted against compounds like **22**, which has the alkenyl group on the amide rather than the aryl ring; its barrier to rotation is about 3 kcal/mol lower. Even **23**, which contains a primary group on nitrogen (allyl) rather than Me, has a barrier 1.5 kcal/mol lower than that for **15b**. With estimated half-lives >20,000 years, atropisomers like **15b**,**f** are essentially indefinitely stable at ambient temperature.

The barrier to rotation of *o*-methoxy substrate **15c** was much lower, $\Delta G^{\ddagger}_{rot} = 26.3$ kcal/mol, and the α-chloro analog **19c** was a little lower still at 25.3 kcal/mol. The 8.1 kcal/mol barrier difference between **15c** and **15b** is significantly larger than expected from related axially chiral systems. For example, Sternhell's model for effects of *ortho*-substituents in biphenyl rotation[32] predicts only a 2–4 kcal/mol difference. The half-lives of the *o*-methoxy analogs are on the order of days at ambient temperature. So rapid room temperature reactions can be conducted with these substrates, but the resolved samples must be stored in the cold.

Chirality Transfer in 6-exo-trig cyclizations

Enantioenriched samples of **15a-c,e-f,h-i** were subjected to optimized reaction conditions for reductive cyclization. The cyclized products were isolated by column chromatography over KF-doped silica, and enantiopurities were determined by chiral HPLC with reference to racemic standards of the product 3,4-dihydroquinolin-2-ones. The results of this series of experiments are shown in Table 3. Both enantiomers of each substrate were tested, and provided identical results within experimental error. Isolated yields of each product were comparable to yields of reactions with racemic substrate (Table 1). The precursor and product enantiomers are correlated in Table 3 by sign of optical rotation, except for **15f**/**14f**, whose absolute configurations are known (see below). Correlation by elution order in the chiral HPLC is provided in the Supporting Information. Unfortunately, there was no obvious correlation between the optical rotation or HPLC elution order of substrates and the respective products of cyclization, so assigning absolute configurations by analogy is not straightforward.

Briefly, the levels of chirality transfer were outstanding in almost all cases, ranging from 92 up to 99%. These high levels were not changed by altering the *N*-substituent (Me or PMB) or the ortho substituent (Me, Br, TMS). Even the samples of **15c** with the *o*-methoxy group cyclized with excellent chirality transfer (94%). The only exception was **15i**, which gave **14i** with a chirality transfer of 80-81% (Entries 13-14). This substrate differs from the others because it lacks an activating group on the alkene and because its R^4 group is Me, not H. Either difference could be responsible for the erosion, as discussed below. These values of chirality transfer in the first examples of "Approach 2" cyclizations are comparable to and usually better than those observed in "Approach 1" room temperature cyclizations of *N*-allyl-*o*-iodoacetamides (74-97%) and *N*-acryloyl-*o*-iodoanilides (49-94%).

The substrate/product pair **15f**/**14f** incorporating an *ortho*-bromine atom was designed to allow assignment of absolute configuration by X-ray crystallography. Unfortunately **15f** did not cooperate. With the goal of making crystalline salts, a sample of (+)-**15f** (99/1 er) was treated with TFA in CH_2Cl_2 producing α,β-unsaturated acid **24** in 71% yield (Figure 8). Salt formation became unnecessary when that acid itself crystallized by slow vapor diffusion method.

Acid **24** crystallized with four unique molecules in the unit cell, as two pairs of dimers displaying hydrogen bonding between the carboxylic acid groups. The differences in geometries between the four structures are small, so only one is shown in Figure 8. In this structure, the plane of the aromatic ring is almost completely orthogonal to the plane of the amide, with a torsion angle of 83°. The alkene acceptor exists in the *s*-trans conformation (an *s*-cis conformation would have significant A-strain), and is twisted slightly out of planarity with the aromatic ring (torsion angle = 156°). Interestingly, the *N*-PMB group is twisted to the same side of the molecule as the α,β-unsaturated carboxylic acid, with their planes nearly parallel. The 3.32–3.86 Å distance range between the two quasi-parallel planes is close to ideal for π-π stacking.[33] Notice that the PMB group shields one face of the alkene. However, this shielding cannot be important in the radical cyclization because the PMB substituent is not essential for high chirality transfer. The absolute configurations of all four molecules in the unit cell were the same, and were assigned by the anomalous scattering method;[34] **24** and accordingly its precursor (+)-**15f** have the (*P*) configuration.

The product **14f** was more cooperative; both the racemate and the pure enantiomers spontaneously solidified on standing. A crystal of (+)-**14f**—the product of cyclization of (+)-**15f**—was grown by vapor phase diffusion and the structure was solved as above; (+)-**14f** has the (*S*) configuration. Two views of this structure are shown in Figure 8. The view on the left is oriented to facilitate comparison with the structure of **15f**. The view on the right, looking into the side of the 3,4-dihydroquinolin-2-one ring, shows how the serious 1,3-interaction between the *N*-PMB group and the *o*-bromine atom is minimized. The angle between these two groups cannot be 90° as in the precursor, and it cannot be 0° as normally preferred for sp^2 hybridized atoms. Instead, a compromise of about 40° is reached because the lactam ring adopts a boat-like conformation that twists the N-aryl bond. This twisting occurs without appreciable pyramidalization at N, and the $CH_2CO_2{}^tBu$ substituent adopts the less-crowded axial-like orientation.

These results validate a working model that is shown in Figure 9. Iodine abstraction by a tributyltin radical from (*P*)-**15f** produces a ground state α-amidoyl radical GS-**16f** that has roughly orthogonal amide and aryl planes as in the precursor. Likewise, the key radical SOMO and the alkene LUMO orbitals are also nearly orthogonal in this ground state of the radical. Coordinated rotation of the *N*-aryl bond, the aryl-alkenyl bond and the $CO–CH_2•$ bond brings the radical to a twisted transition state TS-**16f**. This in turn progresses to the cyclized radical (not shown), and then the cyclized product (*S*)-**14f** after Bu_3SnH reduction.

Production of the enantiomeric product (*R*)-**14f** from radical GS-**16f** requires either that the N–Ar or Ar-alkenyl bond rotates the other way (or alternatively, rotates on past the TS). The former rotation seems unlikely due to the very high barrier. The latter is disfavored because the alkene C=C bond begins to eclipse the N–Ar bond.

In the model shown in Figure 9, the twisting about the NC(O)–CH_2• bond has no stereochemical consequence because a new stereocenter is not formed at the radical carbon atom. That changes if one of the two hydrogen atoms, labeled H^e and H^z in Figure 9, is another group. α-Amidoyl radicals of the general structure NC(O)-CHR• prefer the *s-cis* orientation rather than *s-trans*.[35] In other words, an R group that is appended to radical GS-**16f** alpha to the carbonyl group will take the position of H^e, not H^z. The model TS-**16f** then predicts that a diastereoselective cyclization should occur to give a *trans*-3,4-disubstituted-3,4-dihydroquinolin-2-one.

Single and tandem cyclizations of 2-substituted-α-amidoyl radicals

To test the prediction of diastereoselectivity, we prepared precursor **25** by acylation of PMB-aniline **18c** with racemic 2-bromopropanoyl bromide, as shown in Scheme 2. Precursors **25** have both a chiral axis and a stereocenter, so two racemic diastereomers were produced. These proved to be easily separable by column chromatography and were isolated in yields of 33% and 65%. Each diastereomer was fully characterized, but we could not unambiguously assign relative configurations. Since both diastereomers gave the same products (see below), this ambiguity did not prove to be important in the reaction analysis.

Data for the reductive cyclizations of various isomers of **25** are summarized in Table 4. Racemic samples of **25** were reacted with Bu_3SnH and Et_3B at room temperature according to the usual syringe pump procedure. Both diastereomers gave the single product *trans*-**26** in excellent yield (95-97%). The trans relative configuration was initially assigned based on analysis of coupling constants ($J_{3,4}$ = 14 Hz), and this assignment was later confirmed by crystallography (see below). The cis isomer was not detected.

Next, both samples **25a**,**b** were resolved by chiral HPLC to high enantiopurity, and the four pure stereoisomers were cyclized as usual (Entries 3-6). Yields were reproducibly high (96-98%), and chirality transfers were nearly perfect. The values (99-100%) are even higher than those observed for the primary α-amide radical precursor series. Each enantiomer in a given diastereomeric pair gives a different enantiomer of the product. Across the diastereomeric pairs, (+)-**25a** and (−)-**25b** give the same enantiomer of the product (+)-**26**, so these compounds must have the same configuration in the chiral axis and opposite configurations at the stereocenter. Likewise for the (−)-**25a** and (+)-**25b** pair; each gives (−)-**26**. These results show that the stereoselectivity is dictated by the chiral axis and not the stereocenter. In other words, the diastereomeric pairs of bromides with the same chiral axis configuration provide the same radical. This is sensible since the initially produced radical has sp^2 geometry.[35,36]

Radical cyclizations often proceed with high levels of diastereoselectivity when the radical and alkene acceptor are connected by a pre-formed ring, so we extended the design to incorporate a second cyclization that incorporated new elements of stereoselectivity.[37] The synthesis and cyclizations of tandem precursor **27a-b** are shown in Scheme 3. Racemic 2-bromo-4-pentenoic acid was converted to the acid chloride, which was used to acylate **18c**. This produced diastereomers **27a** (35% yield) and **27b** (39% yield) that were separated by column chromatography. Again, the relative configurations of **27a,b** were not assigned.

Tandem cyclization of a single enantiomer of **27** can give as many as 16 stereoisomers of **28**; however, we already know that racemization will not occur and that the first cyclization should be highly diastereoselective for the *trans* isomer. This reduces to four the number of likely

product isomers. Since we already understood the effect of the relative stereochemistry from the experiments in Table 3, we cyclized one of the diastereomers of **27** as a racemate, and resolved the other prior to cyclization.

Racemic **27a** was treated with Bu_3SnH under syringe pump conditions at room temperature (Scheme 3). After column chromatography, tricyclic product *rac*-**28** was isolated in 51% yield as a single diastereomer. Other fractions of side products contained, among other unidentified compounds, two minor diastereomers of the 6-*endo*-*trig*/5-*exo*-*trig* sequence, as evidenced by two distinct doublets in the upfield region denoting the respective methyl signals of the diastereomers. Enantiopure samples of **27b** were accessed by resolution with chiral HPLC, and were also subjected to the reaction conditions. These reactions provided the same diastereomer but opposite enantiomers of **28** in similar yields and excellent chirality transfer (98-99%).

Because the minor products and various impurities were inseparable from each other, it was not possible to characterize any of the secondary products or to provide an accurate measure of the diastereoselectivity in the second cyclization. However, we conservatively estimate that none of the minor products exceeded 10% of the mixture, so the second cyclization must also be reasonably diastereoselective (≥4/1).

The structure of *rac*-**28** was established by X-ray crystallography, and a diagram is shown in Figure 10. The ring fusion is *trans*,[38] and $J_{3,4}$ is again 14.1 Hz with a dihedral angle H^3–C^3–C^4–H^4 of 176° in the crystal. This confirms the assignment of *trans* relative configuration of **26** above.

Models for the first and second cyclizations of the radicals generated from **27** are shown in Figure 11. The model for the first cyclization, which also serves for the radical derived from **25**, follows directly from the model for the primary radical (Figure 9). The alkyl group on the radical center (R = Me or $CH_2CH{=}CH_2$) orients itself *s*-*cis* to the anilide carbonyl group. Then, twisting as indicated in **TS-29** directs the first cyclization with control of both relative and absolute configuration. The structure of the major isomer **28** formed in the second cyclization follows directly from the Beckwith-Houk model[39] of a chair-like transition state **TS-30** with equatorial-like substituents on the forming ring. The minor products can arise from a chair-like transition state with the radical substituent in a quasi-axial orientation, or boat-like transition states with either axial or equatorial orientations. In flexible systems, the chair and boat can flip to provide additional possible geometries, but the rigidity of the ring fusion to the 3,4-dihydroquinolone ring prevents that flip in this case.

Conclusions

Radical cyclizations (Bu_3SnH, Et_3B/air, rt) of an assortment of α-halo-*ortho*-alkenyl anilides provide 3,4-dihydroquinolin-2-ones in high yield. The precursors are axially chiral (stable atropisomers) but the products are not. Cyclizations of enantioenriched precursors occur with transfer of axial chirality to the new stereocenter of the products with exceptionally high fidelity (often > 95%). Single and tandem cyclizations of α-halo-*ortho*-alkenyl anilides bearing an additional substituent on the α-carbon occur with both high chirality transfer and high diastereoselectivity. Overall, the new method is an attractive route for stereoselective synthesis of diverse 3,4-dihydroquinolin-2-ones.

Crystal structures have been used to rigorously assign configurations of one precursor and two products. Straightforward models interpret both the chirality transfer and diastereoselectivity aspects, reinforcing the notion that predictions of stereochemical outcomes of reactions of axially chiral amides are both easy and reliable.

Prior reactions with axial chirality transfer in the anilide series have featured reactive intermediates (radicals, anions, transition metals) on the aryl ring of the anilide and acceptors in the amide. This first-in-class example of the reverse approach suggests broad potential for axial chirality transfer from assorted reactive intermediates in the amide to acceptors on the aryl ring.

Supplementary Material

Refer to Web version on PubMed Central for supplementary material.

Acknowledgments

We thank the National Science Foundation for funding this work and the National Institutes of Health for a grant to purchase an NMR spectrometer.

References and Footnotes

1. For a more complete collection of references to biologically active 3,4-dihydroquinolin-2-ones and methods of synthesis, see: Zhou W, Zhang L, Jiao N. Tetrahedron 2009;65:1982–1987.
2. Ito C, Itoigawa M, Otsuka T, Tokuda H, Nishino H, Furukawa H. J. Nat. Prod 2000;63:1344–1348. [PubMed: 11076549]
3. Kimura Y, Kusano M, Koshino H, Uzawa J, Fujioka S, Tani K. Tetrahedron Lett 1996;37:4961–4964.
4. (a) Ellis D, Kuhen KL, Anaclerio B, Wu B, Wolff K, Yin H, Bursulaya B, Caldwell J, Karanewsky D, He Y. Bioorg. Med. Chem. Lett 2006;16:4246–4251. [PubMed: 16782337] (b) Patel M, McHugh RJ Jr. Cordova BC, Klabe RM, Bacheler LT, Erickson-Viitanen S, Rodgers JD. Bioorg. Med. Chem. Lett 2001;11:1943–1945. [PubMed: 11459666]
5. Seitz W, Geneste H, Backfisch G, Delzer J, Graef C, Hornberger W, Kling A, Subkowskic T, Norbert Z. Bioorg. Med. Chem. Lett 2008;18:527–531. [PubMed: 18068982]
6. (b) Bernauer K, Englert G, Vetter W, Weiss E. Helv. Chim. Acta 1969;52:1886–1905. c) Oberhänsli WE. Helv. Chim. Acta 1969;52:1905–1911. d) Plat M, Hachem-Mehri M, Koch M, Scheidegger U, Potier P. Tetrahedron Lett 1970;39:3395–3398.Isolation: Bernauer K, Englert G, Vetter W. Experientia 1965;21:374–375. [PubMed: 5871070]
7. (b) Denmark SE, Cottell JJ. Adv. Synth. Catal 2006;348:2397–2042. c) Selig P, Bach T. Angew. Chem. Int. Ed 2008;47:5082–5084. d) Selig P, Herdtweck E, Bach T. Chem. Eur. J 2009;15:3509–3525.Synthesis: Overman LE, Robertson GM, Robichaud AJ. J. Am. Chem. Soc 1991;113:2598–2610.
8. (a) El Ali B, Okuro K, Vasapollo G, Alper H. J. Am. Chem. Soc 1996;118:4264–4270. (b) Dong C, Alper H. Tetrahedron: Asymmetry 2004;15:35–40. (c) Okuro K, Kai H, Alper H. Tetrahedron: Asymmetry 1997;8:2307–2309. (d) Blay G, Cardona L, Torres L, Pedro JR. Synthesis 2007:108–112. e) Bolm C, Hildebrand JP. Tetrahedron Lett 1998;39:5731–5734.
9. Other radical approaches include bimolecular additions, see reference 1, and cyclizations to isocyanates, see: Minin PL, Walton JC. J. Org. Chem 2003;68:2960–2963. [PubMed: 12662077]
10. (a) Clark AJ, Jones K, McCarthy C, Storey JMD. Tetrahedron Lett 1991;32:2829–2832. (b) Clark AJ, Jones K. Tetrahedron 1992;48:6875–6882. (c) Lopez de Turiso FG, Curran DP. Org. Lett 2005;7:151–154. [PubMed: 15625000]Related additions to aryl rings
11. (a) Sato T, Ishida S, Ishibashi H, Ikeda M. J. Chem. Soc. Perk. Trans. 1 1991:353–359. (b) Ishibashi H, Sato T, Ikeda M. Synthesis 2002;6:695–713.
12. Allan GM, Parsons AF, Pons J-F. Synlett 2002:1431–1434.
13. McAllister LA, Turner KL, Brand S, Stefaniak M, Procter DJ. J. Org. Chem 2006;71:6497–6507. [PubMed: 16901135]
14. (a) Oki M. Allinger NL, Eliel E, Wilen SH. Top. Stereochem 1983;14:1–81.(b) Oki, M. The Chemistry of Rotational Isomers. Springer-Verlag; New York: 1993. (c) Wolf, C. Dynamic Stereochemistry of Organic Compounds. RSC Publishing; Cambridge, UK: 2008.
15. (a) Curran DP, Hale GR, Geib SJ, Balog A, Cass QB, Degani ALG, Hernandes MZ, Freitas LCG. Tetrahedron: Asymmetry 1997;8:3955–3975. (b) Adler T, Bonjoch J, Clayden J, Font-Bardía M,

Pickworth M, Solans X, Solé D, Vallverdú L. Org. Biomol. Chem 2005;3:3173–3183. [PubMed: 16106298] (c) Petit M, Lapierre AJB, Curran DP. J. Am. Chem. Soc 2005;127:14994–14995. [PubMed: 16248616]

16. (a) Curran DP, Qi H, Geib SJ, DeMello NC. J. Am. Chem. Soc 1994;116:3131–3132. (b) Curran DP, Liu WD, Chen CH-T. J. Am. Chem. Soc 1999;121:11012–11013. (c) Ates A, Curran DP. J. Am. Chem. Soc 2001;123:5130–5131. [PubMed: 11457357] (d) Curran DP, Chen CHT, Geib SJ, Lapierre AJB. Tetrahedron 2004;60:4413–4424. (e) Petit M, Geib SJ, Curran DP. Tetrahedron 2004;60:7543–7552.
17. Guthrie DB, Curran DP. Org. Lett 2009;11:249–251. [PubMed: 19055374]
18. Lapierre AJB, Geib SJ, Curran DP. J. Am. Chem. Soc 2007;129:494–495. [PubMed: 17227004]
19. Curran DP, Abraham AC, Liu HT. J. Org. Chem 1991;56:4335–4337.
20. Opatz T, Ferenc D. Org. Lett 2006;8:4473–4475. [PubMed: 16986928]
21. Jeffery T. Tetrahedron 1996;52:10113–10130.
22. Campbell JB Jr. Firor JW, Davenport TW. Synth. Commun 1989;19:2265–2272.
23. Yorimitsu, H.; Oshima, K. Radicals in organic synthesis. Renaud, P.; Sibi, MP., editors. Vol. 1. Wiley-VCH; Weinheim: 2001. p. 11-27.
24. Harrowven DC, Guy IL. Chem. Commun 2004:1968–1969.
25. Franz JA, Suleman NK, Alnajjar MS. J. Org. Chem 1986;51:19–25.
26. Stork G, Mah R. Heterocycles 1989;28:723–727.
27. (a) Newcomb M. Tetrahedron 1993;49:1151–1176.(b) Newcomb, M. Radicals in Organic Synthesis. Vol. 1st ed.. Renard, P.; Sibi, M., editors. Vol. 1. Wiley-VCH; Weinheim: 2001. p. 317-336.
28. (a) Chatgilialoglu C, Dickhaut J, Giese B. J. Org. Chem 1991;56:6399–6403. (b) Chatgilialoglu C, Ingold KU, Scaiano JC. J. Am. Chem. Soc 1981;103:7739–7742.
29. Hanessian S, Dhanoa DS, Beaulieu PL. Can. J. Chem 1987;65:1859.
30. Stewart WE, Siddall TH. Chem. Rev 1970;70:517–551.
31. (a) Chupp JP, Olin JF. J. Org. Chem 1967;32:2297–2303. (b) Ototake N, Taguchi T, Kitagawa O. Tetrahedron Lett 2008;49:5458–5460. (c) Nobutaka O, Masashi N, Yasuo D, Haruhiko F, Osamu K. Chem. Eur. J 2009;15:5090–5095.
32. Bott G, Field LD, Sternhell S. J. Am. Chem. Soc 1980;102:5618–5626.
33. (a) Maddaluno JF, Gresh N, Giessner-Prettre C. J. Org. Chem 1994;59:793–802. (b) Roesky HW, Andruh M. Coord. Chem. Rev 2003;236:91–119.
34. Dunitz JD. Angew. Chem. Int. Ed 2001;40:4167–4173.
35. Porter NA, Giese B, Curran DP. Acc. Chem. Res 1991;24:296–304.
36. Musa OM, Choi SY, Horner JH, Newcomb M. J. Org. Chem 1998;63:786–793. [PubMed: 11672074] Interestingly, however, the rate of rotation of rotation about the NC(O)-CHMe(•) may be similar to or possibly even slower than the rate of radical cyclization. If that is the case, then both diastereomers of precursor must produce the same s-*cis* radical. For rotation rate information see: Strub W, Roduner E, Fischer H. J. Phys. Chem 1987;91:4379–4383.
37. Curran, DP.; Porter, NA.; Giese, B. Stereochemistry of Radical Reactions: Concepts, Guidelines, and Synthetic Applications. VCH Publishers, Inc.; New York: 1996. p. 30-82.see especially
38. Akritopoulou-Zanze I, Whitehead A, Waters JE, Henry RF, Djuric SW. Tetrahedron Lett 2007;48:3549–3552.
39. Spellmeyer DC, Houk KN. J. Org. Chem 1987;52:959–974.Beckwith ALJ, Schiesser CH. Tetrahedron Lett 1985;26:373–376.

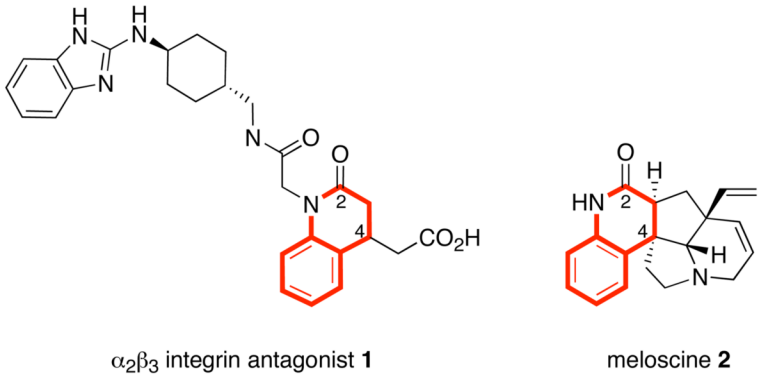

$\alpha_2\beta_3$ integrin antagonist **1** meloscine **2**

Figure 1.
Representative 3,4-dihydroquinolin-2-ones with ring system highlighted in red

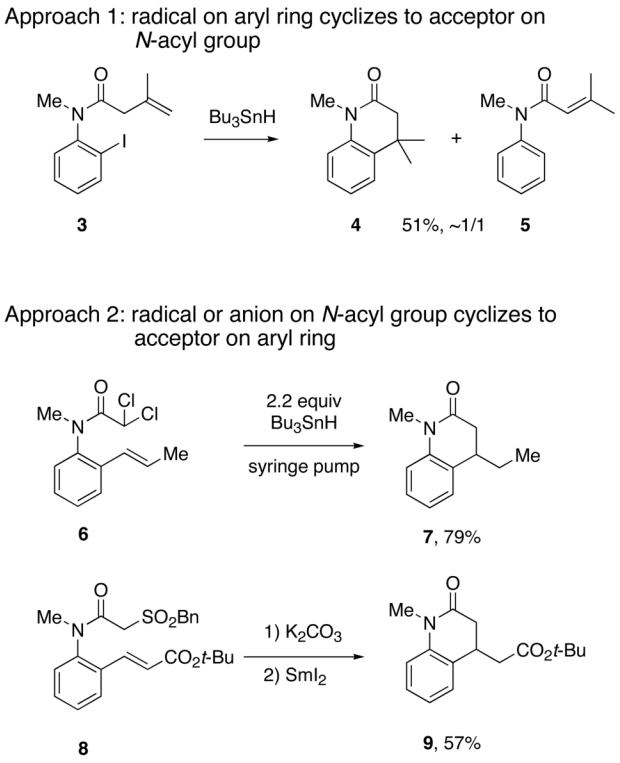

Figure 2.
Two 6-*exo*-*trig* cyclization approaches to racemic dihydroquinolin-2-ones

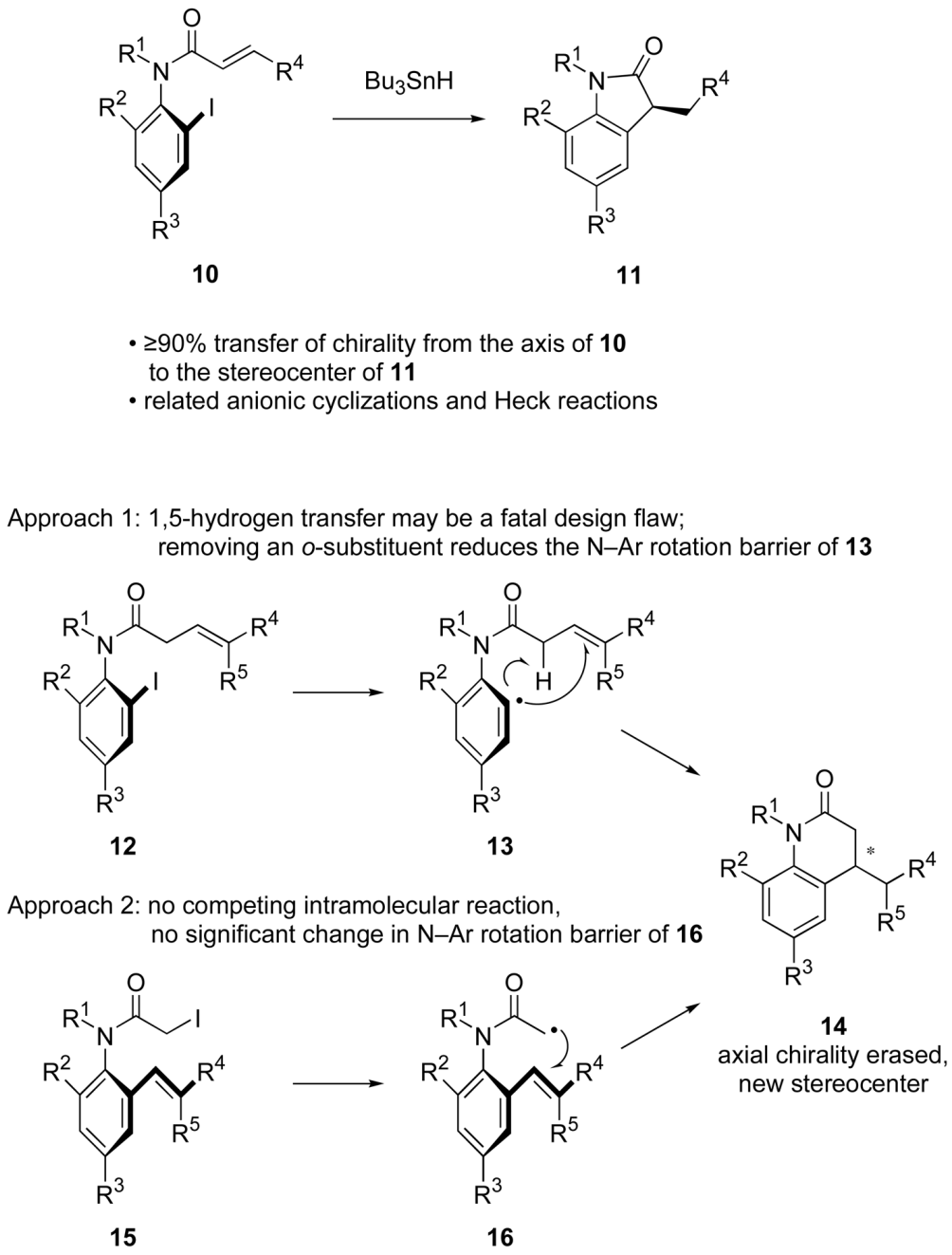

Figure 3.
Established approach to indol-2-ones (top) compared to two potential approaches to dihydroquinolin-2-ones (bottom)

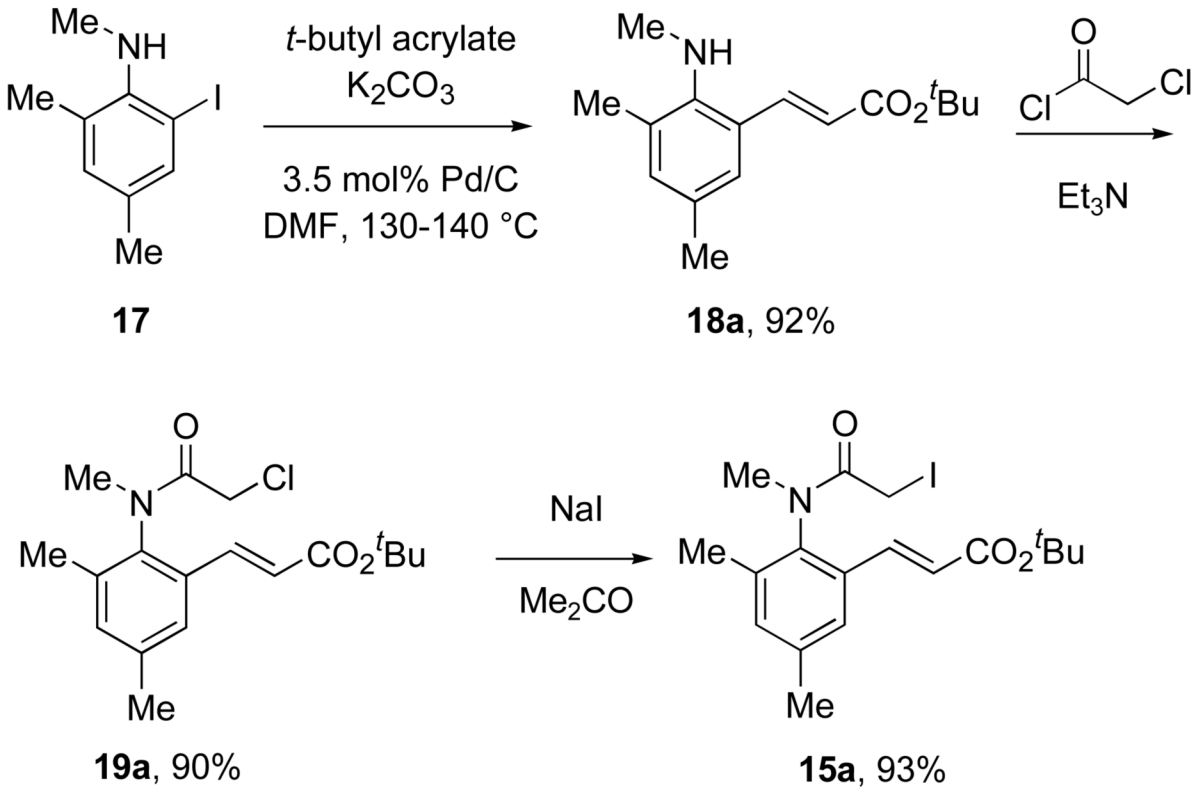

Scheme 1.
Typical synthesis of a radical cyclization precursor illustrated with **15a**

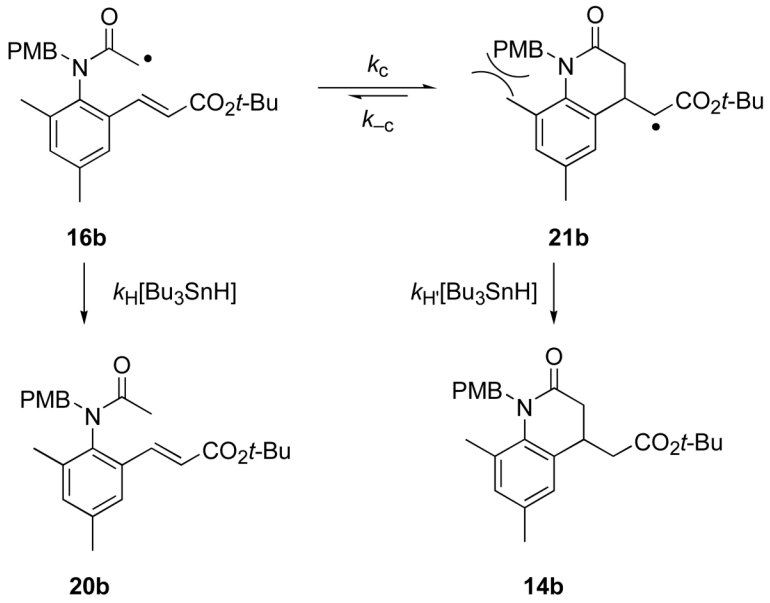

Figure 4.
Mechanistic framework for rate constant measurements

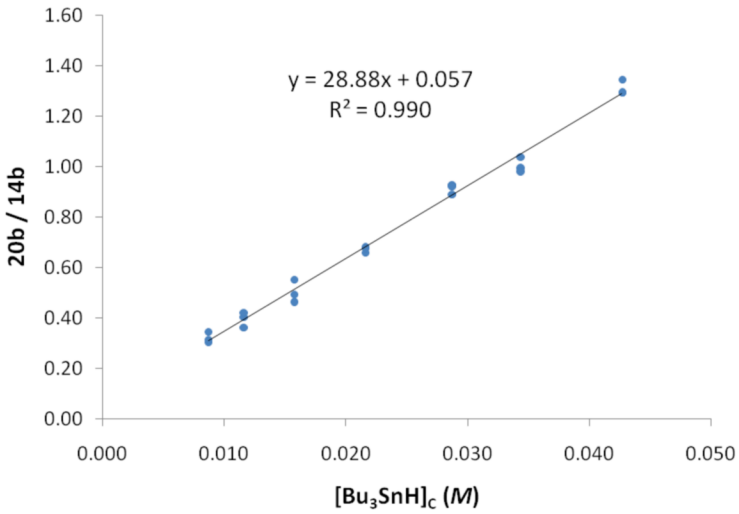

Figure 5.
Kinetic competition plot of the data in Table 2 for reactions of radical **16b**

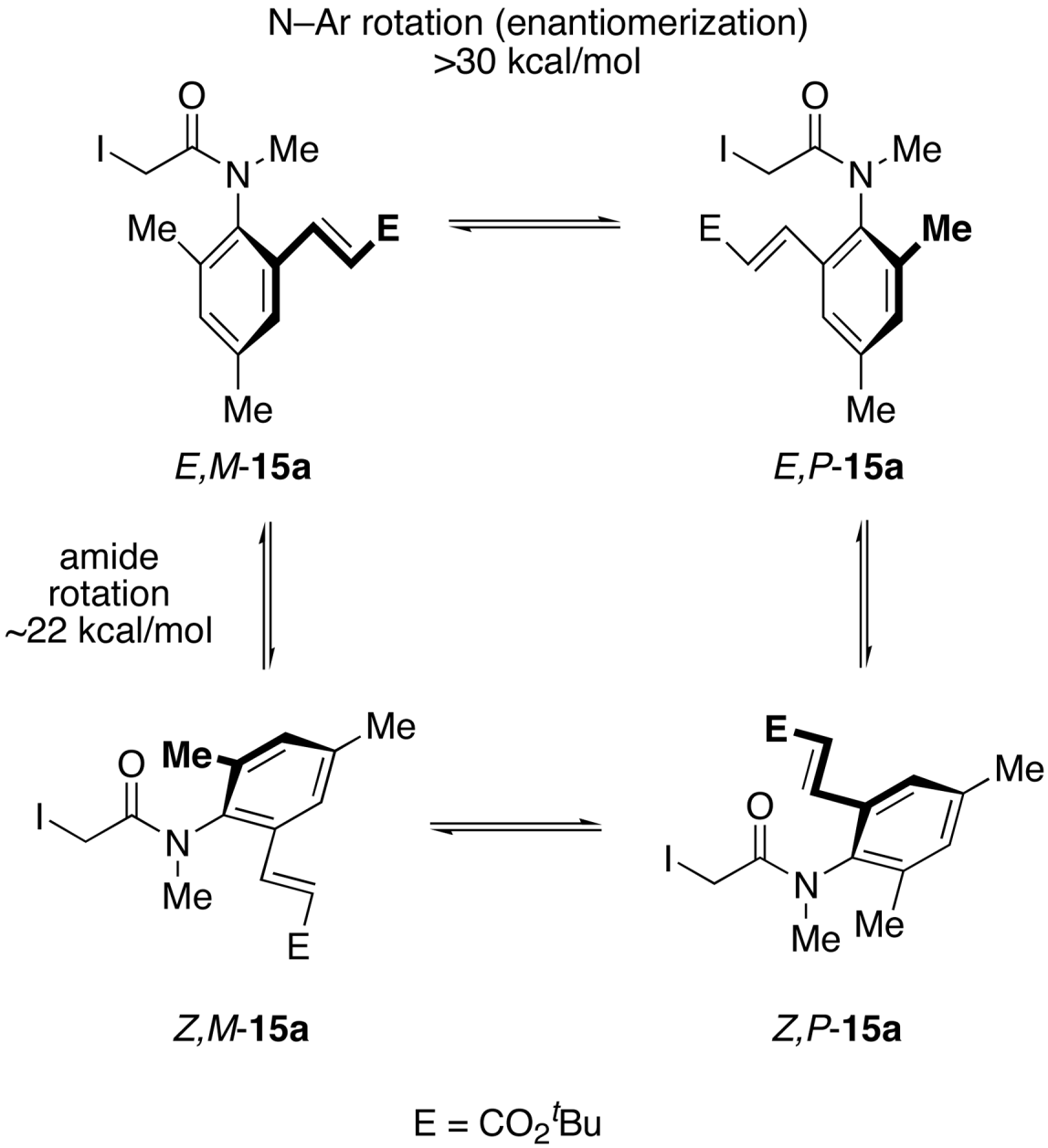

Figure 6.
Rotational dynamics of *N*-methyl anilide **15a**

new barriers

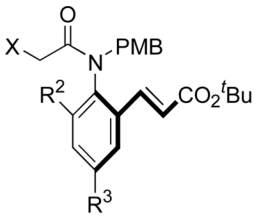

cmpd	X	R^2	R^3	$\Delta G^{\ddagger}$, kcal/mol
15b	I	Me	Me	34.3
15f	I	Br	Me	34.2
15c	I	OMe	H	26.2
19c	Cl	OMe	H	25.3

benchmarks

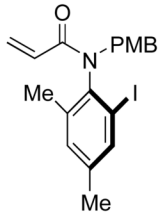

22, $\Delta G^{\ddagger}$ = 30.8 kcal/mol

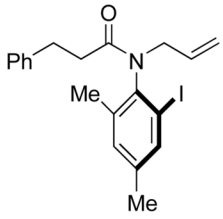

23, $\Delta G^{\ddagger}$ = 32.7 kcal/mol

Figure 7.
Measured rotation barriers for amides **15** and **19** along with literature benchmarks **22** and **23**

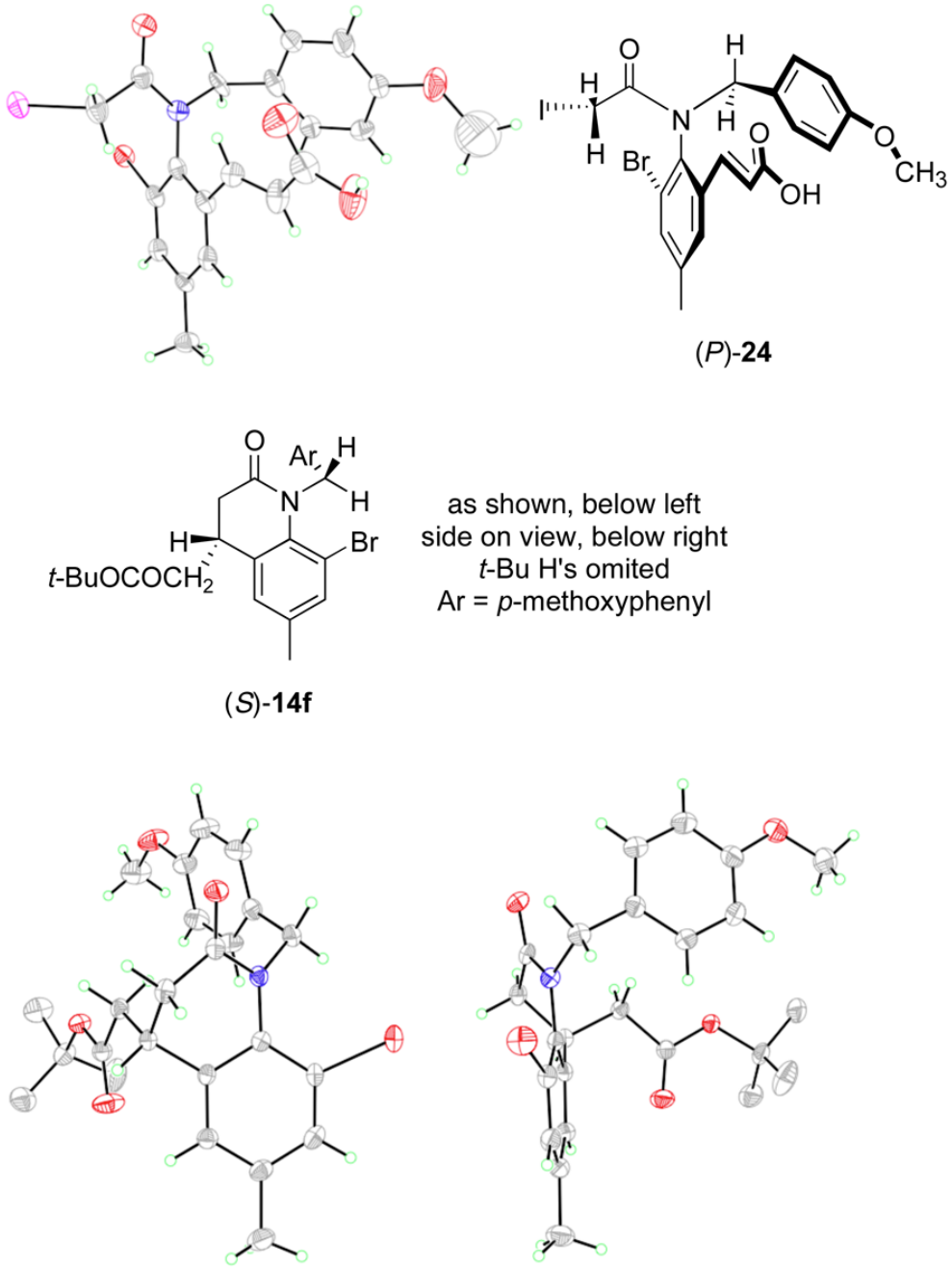

Figure 8.
X-ray crystal structures of (*P*)-**24** (top) and **14f** (bottom, with front and side views)

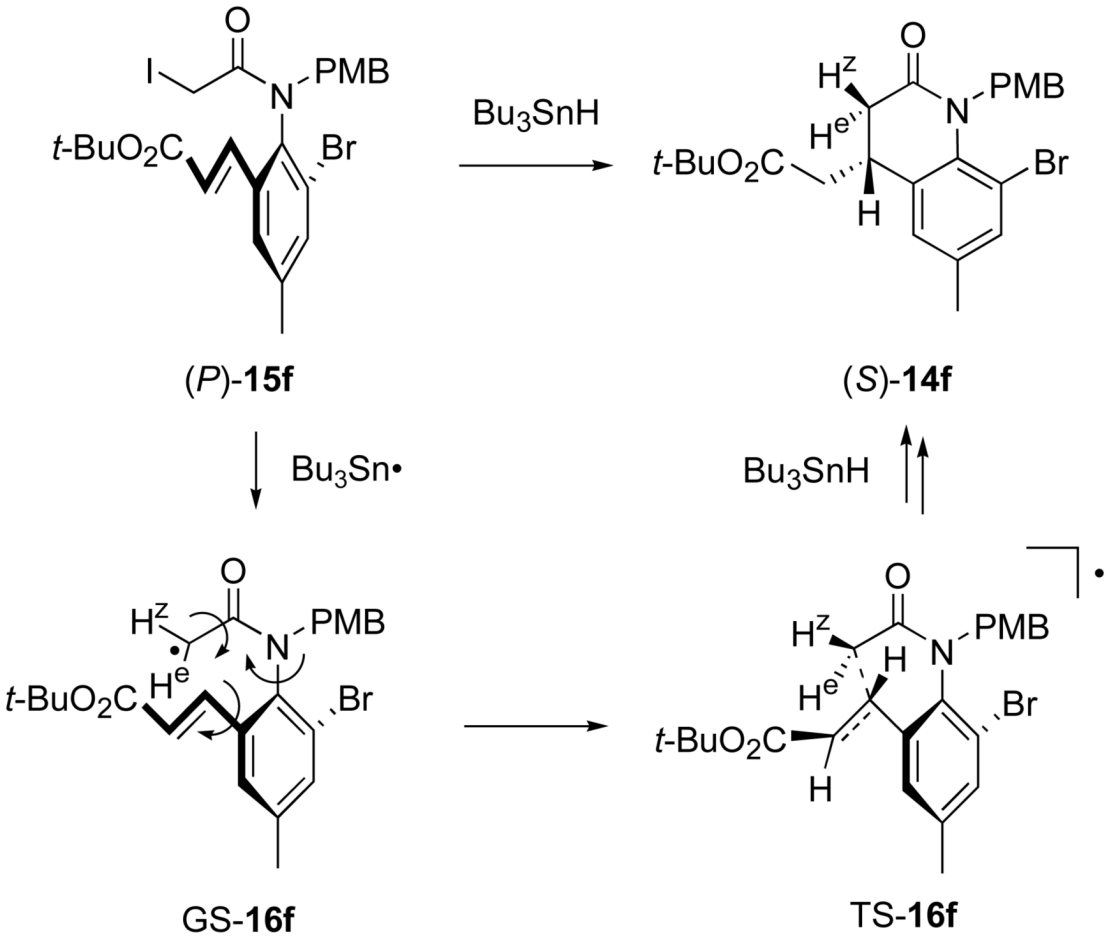

Figure 9.
Model for chirality transfer illustrated with **15f**

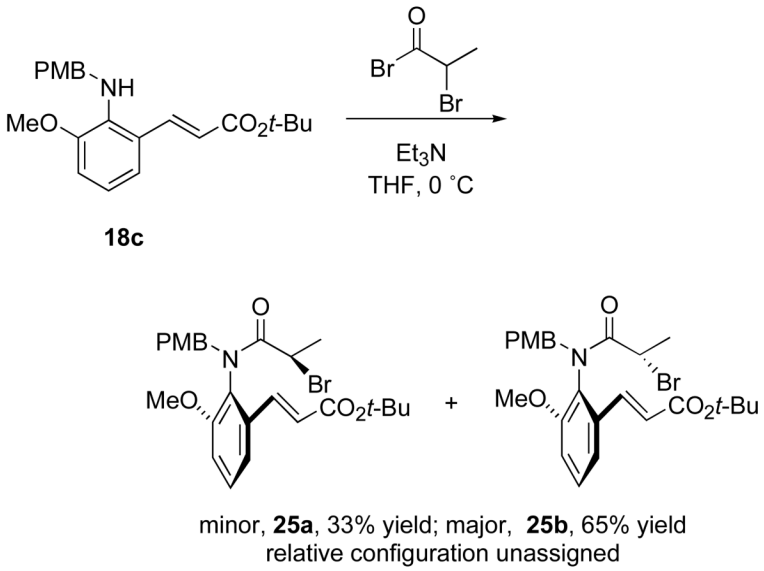

Scheme 2.
Synthesis and separation of two diastereomers of precursor **25**

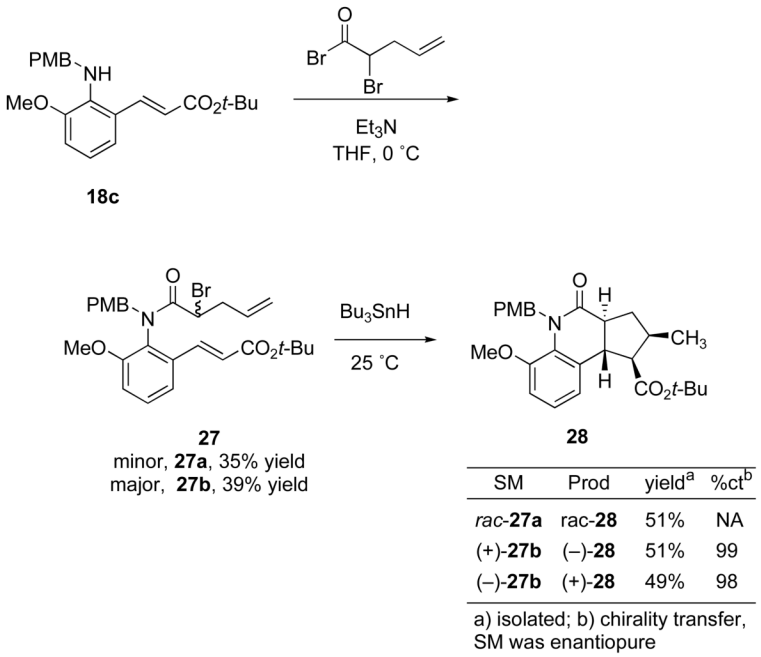

SM	Prod	yield[a]	%ct[b]
rac-**27a**	rac-**28**	51%	NA
(+)-**27b**	(–)-**28**	51%	99
(–)-**27b**	(+)-**28**	49%	98

a) isolated; b) chirality transfer, SM was enantiopure

Scheme 3.
Synthesis and cyclization of tandem precursor **27**

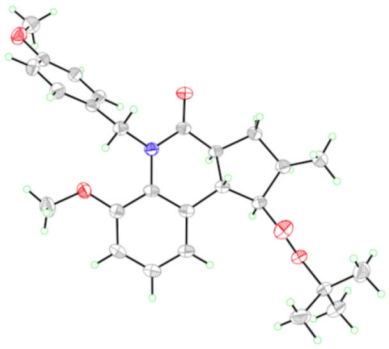

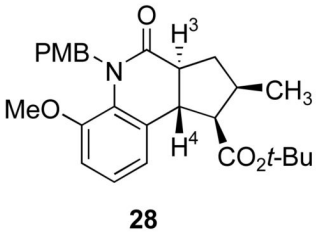

28

Figure 10.
X-ray crystal structure of tricycle **28**

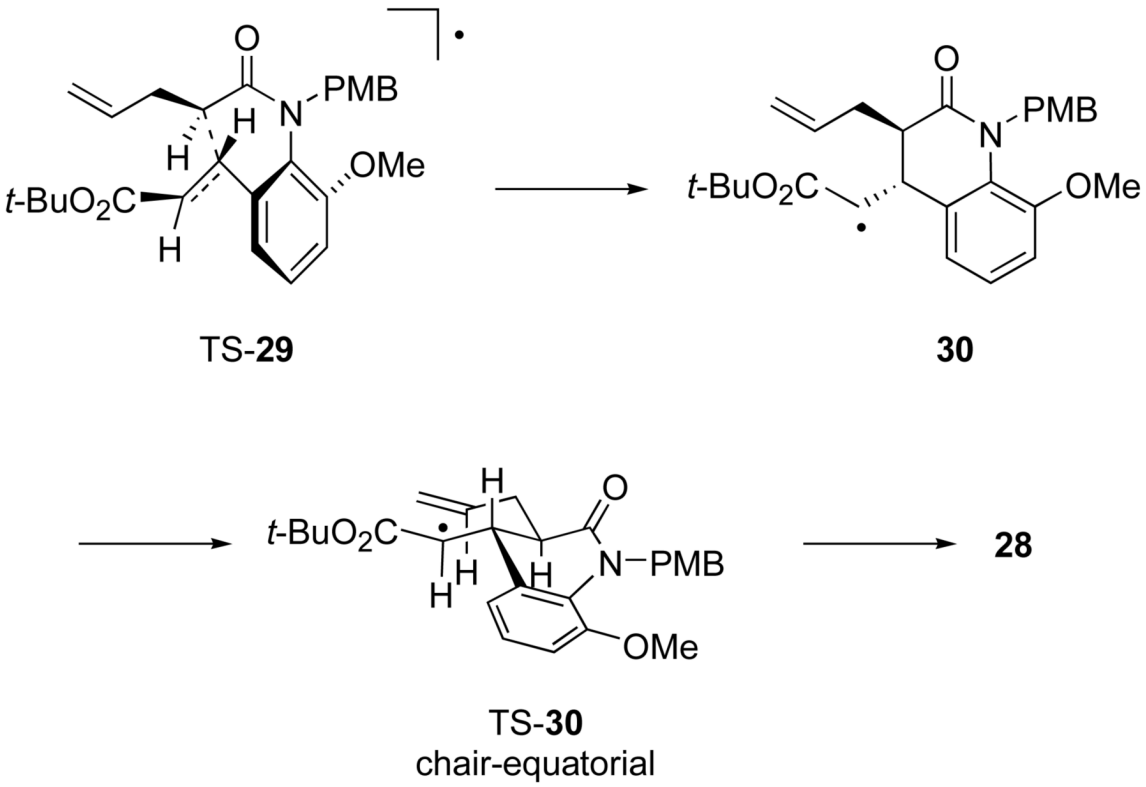

Figure 11.
Models of first and second cyclizations of radicals derived from **27**

Table 1

Isolated yields of radical cyclization products **14a-i** from racemic precursors **15a-i**[a]

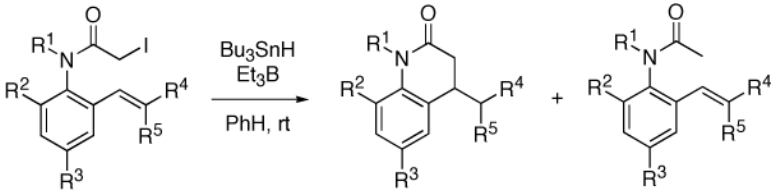

rac-**15a-i** *rac*-**14a-i** *rac*-**20a-i**

entry	α-I	R^1	R^2	R^3	R^4	R^5	% yield[b]
1	**15a**	Me	Me	Me	CO_2t-Bu	H	83
2	**15b**	PMB	Me	Me	CO_2t-Bu	H	85
3	**15c**	PMB	OMe	H	CO_2t-Bu	H	97
4	**15d**	Ts	Me	Me	CO_2t-Bu	H	nd[c,d]
5	**15e**	PMB	TMS	Me	CO_2t-Bu	H	93
6	**15f**	PMB	Br	Me	CO_2t-Bu	H	61
7	**15g**	PMB	Me	Me	4-BrC_6H_4	H	nd[c]
8	**15h**	PMB	Me	Me	CN	H	< 70[d]
9	**15i**	PMB	Me	Me	Me	Me	51[e]

[a] Conditions: Bu_3SnH and Et_3B in 20 mL PhH were added over 2 h via syringe to a 10 mM PhH solution of **15**.

[b] Yield of racemic **14** after isolation by column chromatography on 10% w/w KF/silica gel.

[c] nd = Not determined.

[d] Fixed concentration of Bu_3SnH at 5 mM.

[e] Directly reduced **20** was detected in crude reaction mixture by TLC or ^1H NMR.

Table 2

Summary of results of competition experiments with **15b**

[Bu_3SnH][a]	% yld 14b[b]	% yld 20b[b]	total yld	red : cyc[d]
14.9 mM	67	21	89	24 : 76
19.9 mM	64	25	89	28 : 72
27.0 mM	59	30	88	33 : 67
37.0 mM	58	39	97	40 : 60
49.2 mM	50	46	95	48 : 52
58.8 mM	45	45	90	50 : 50
73.2 mM	33	43	76	57 : 43

[a] initial concentration.

[b] GC yield, using eicosane as an internal standard. Yields are an average of three trials.

[c] The ratio of reduced **20b** to cyclized **14b**.

Table 3

Yields and chirality transfer levels in cyclizations of enantiomeric precursors **15** to give **14**[a]

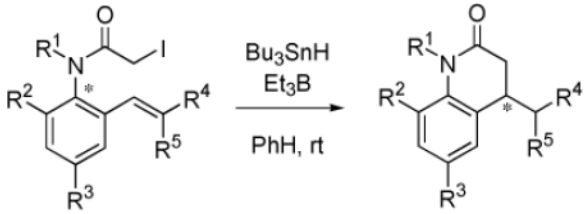

15a-i **14a-i**

entry	precursor	R^1	R^2	R^3	R^4	R^5	er	% yield 14[b]	er	% ct[e]
1	(+)-**15a**	Me	Me	Me	CO_2t-Bu	H	98.5/1.5	79	91/9	92
2	(−)-**15a**	Me	Me	Me	CO_2t-Bu	H	85/15	81	84/16	99
3	(+)-**15b**	PMB	Me	Me	CO_2t-Bu	H	100/0	87	95/5	95
4	(−)-**15b**	PMB	Me	Me	CO_2t-Bu	H	100/0	85	96/4	96
5	(+)-**15c**	PMB	OMe	H	CO_2t-Bu	H	99/1	94	93/7	94
6	(−)-**15c**	PMB	OMe	H	CO_2t-Bu	H	99/1	96	93/7	94
7	(+)-**15e**	PMB	TMS	Me	CO_2t-Bu	H	100/0	95	95/5	95
8	(−)-**15e**	PMB	TMS	Me	CO_2t-Bu	H	100/0	93	94/6	96
9	(*P*)-**15f**	PMB	Br	Me	CO_2t-Bu	H	99/1	63	95/5	96
10	(*M*)-**15f**	PMB	Br	Me	CO_2t-Bu	H	0/100	66	94/6	94
11	(+)-**15h**	PMB	Me	Me	CN	H	99.5/0.5	71	93/7	93[e]
12	(−)-**15h**	PMB	Me	Me	CN	H	99/1	68	96/4	97[e]
13	(+)-**15i**	PMB	Me	Me	Me	Me	99/1	57	80/20	81
14	(−)-**15i**	PMB	Me	Me	Me	Me	0/100	55	80/20	80

[a] Conditions: Bu_3SnH and Et_3B in 20 mL PhH were added over 2 h via syringe pump to a stirred 10 mM PhH solution of **15**.

[b] Yield of **14** after isolation by column chromatography on 10% w/w KF/silica gel.

[c] Absolute configuration determined by X-ray crystallography.

[d] Percent chirality transfer.

[e] Neat Bu_3SnH and Et_3B were added sequentially in one portion to a stirred PhH solution of iodide with $[Bu_3SnH]_i$ = 5 mM.

J Am Chem Soc. Author manuscript; available in PMC 2010 October 28.

Table 4

Cyclizations of secondary radical precursor **25** to **26**

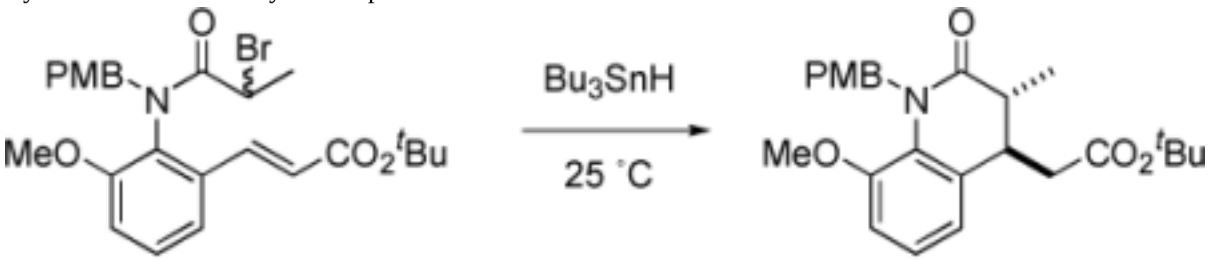

25a,b *trans*-**26**

entry	substrate	er	product	% yield[a]	er	% chirality transfer
1	*rac*-**25a**	50/50	*rac*-**26**	95	50/50	N/A
2	*rac*-**25b**	50/50	*rac*-**26**	97	50/50	N/A
3	(+)-**25a**	98/2	(+)-**26**	98	98/2	100
4	(−)-**25a**	99/1	(−)-**26**	96	98/2	99
5	(+)-**25b**	100/0	(−)-**26**	98	99/1	99
6	(−)-**25b**	100/0	(+)-**26**	97	99.5/0.5	99.5

[a]Yield after isolation by column chromatography on 10% w/w KF/silica gel.